Science of the Total Environment 645 (2018) 192–204

Contents lists available at ScienceDirect

Science of the Total Environment

journal homepage: www.elsevier.com/locate/scitotenv

Retention and remobilization mechanisms of environmentally aged silver nanoparticles in an artificial riverbank filtration system

Laura Degenkolb [a,b,*], George Metreveli [c], Allan Philippe [c], Anja Brandt [d], Kerstin Leopold [d], Lisa Zehlike [a,b], Hans-Jörg Vogel [e], Gabriele E. Schaumann [c], Thomas Baumann [f], Martin Kaupenjohann [a], Friederike Lang [g], Samuel Kumahor [e], Sondra Klitzke [a,b,g]

[a] Berlin University of Technology, Institute of Ecology, Department of Soil Science, Ernst-Reuter Platz 1, 10587 Berlin, Germany
[b] German Environment Agency, Section Drinking Water Treatment and Resource Protection, Schichauweg 58, 12307 Berlin, Germany
[c] University of Koblenz-Landau, Institute for Environmental Sciences, Group of Environmental and Soil Chemistry, Fortstraße 7, 76829 Landau, Germany
[d] Ulm University, Institute of Analytical and Bioanalytical Chemistry, Albert-Einstein-Allee 11, 89081 Ulm, Germany
[e] Helmholtz Centre for Environmental Research Leipzig-Halle, Department of Soil Physics, Theodor-Lieser-Strasse 4, 06120 Halle, Germany
[f] Technical University of Munich, Institute of Hydrochemistry, Marchioninistr. 17, 81377 München, Germany
[g] Albert-Ludwigs-Universität Freiburg, Chair of Soil Ecology, Alte Universität, Bertoldstraße 17, 79098 Freiburg i. Br., Germany

HIGHLIGHTS

- Outdoor, large-scale column experiments and laboratory batch studies
- Strong retention of Ag NP, but highest mobility of soil-aged Ag NP
- 50% of retained Ag is remobilizable by mechanical forces and hydrochemical changes.
- NOM and ionic strength reduction enhances NP mobility, Ca reduces it.
- Co-mobilization with natural colloids is an important remobilization mechanism.

GRAPHICAL ABSTRACT

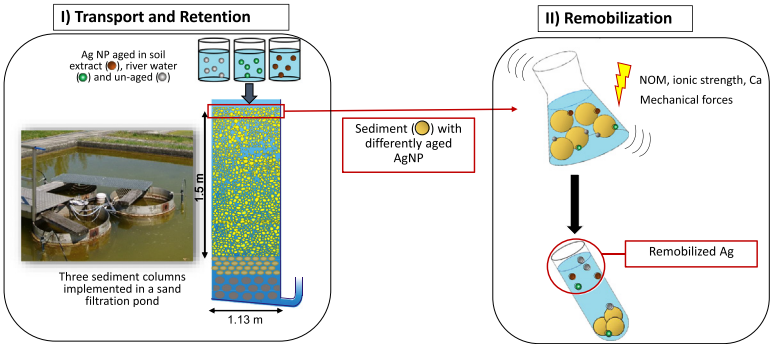

ARTICLE INFO

Article history:
Received 18 May 2018
Received in revised form 6 July 2018
Accepted 6 July 2018
Available online 17 July 2018

Editor: D. Barcelo

Keywords:
Heteroaggregation
Nanoparticle transformation
Breakthrough

ABSTRACT

Riverbank filtration systems are important structures that ensure the cleaning of infiltrating surface water for drinking water production. In our study, we investigated the potential risk for a breakthrough of environmentally aged silver nanoparticles (Ag NP) through these systems. Additionally, we identified factors leading to the remobilization of Ag NP accumulated in surficial sediment layers in order to gain insights into remobilization mechanisms.

We conducted column experiments with Ag NP in an outdoor pilot plant consisting of water-saturated sediment columns mimicking a riverbank filtration system. The NP had previously been aged in river water, soil extract, and ultrapure water, respectively. We investigated the depth-dependent breakthrough and retention of NP. In subsequent batch experiments, we studied the processes responsible for a remobilization of Ag NP retained in the upper 10 cm of the sediments, induced by ionic strength reduction, natural organic matter (NOM), and mechanical forces. We determined the amount of remobilized Ag by ICP-MS and differentiated between particulate

* Corresponding author at: German Environment Agency, Section Drinking Water Treatment and Resource Protection, Schichauweg 58, 12307 Berlin, Germany.
E-mail addresses: laura.degenkolb@uba.de (L. Degenkolb), metreveli@uni-landau.de (G. Metreveli), philippe@uni-landau.de (A. Philippe), anja.brandt@uni-ulm.de (A. Brandt), kerstin.leopold@uni-ulm.de (K. Leopold), lisa.zehlike@uba.de (L. Zehlike), hans-joerg.vogel@ufz.de (H.-J. Vogel), schaumann@uni-landau.de (G.E. Schaumann), tbaumann@tum.de (T. Baumann), martin.kaupenjohann@tu-berlin.de (M. Kaupenjohann), fritzi.lang@bodenkunde.uni-freiburg.de (F. Lang), samuel.kumahor@ufz.de (S. Kumahor), sondra.klitzke@uba.de (S. Klitzke).

https://doi.org/10.1016/j.scitotenv.2018.07.079

Mobility
Reversibility

and ionic Ag after remobilization using GFAAS. The presence of Ag-containing heteroaggregates was investigated by combining filtration with single-particle ICP-MS.
Single and erratic Ag breakthrough events were mainly found in 30 cm depth and Ag NP were accumulated in the upper 20 cm of the columns. Soil-aged Ag NP showed the lowest retention of only 54%. Remobilization was induced by the reduction of ionic strength and the presence of NOM in combination with mechanical forces. The presence of calcium in the aging- as well as the remobilizing media reduced the remobilization potential. Silver NP were mainly remobilized as heteroaggregates with natural colloids, while dissolution played a minor role.
Our study indicates that the breakthrough potential of Ag NP in riverbank filtration systems is generally low, but the aging in soil increases their mobility. Remobilization processes are associated to co-mobilization with natural colloids.

1. Introduction

Riverbank filtration systems are natural systems that may ensure the cleaning of surface water for recharging groundwater. Due to their natural cleaning capacity, i.e. through mechanical filtering, sorption, and biodegradation processes, these systems have become increasingly important for drinking water production (Sprenger et al., 2017). The effectiveness of riverbank filtration in removing microorganisms such as pathogens (i.e. bacteria and viruses) from infiltrating surface water has long been recognized in Germany (Schmidt et al., 2003). Nowadays, there is a much larger number of potential pollutants in anthropogenically influenced water bodies which need to be removed before drinking water usage (Schmidt et al., 2003). One example is nanoparticles (NP) which are included in many industrial applications and consumer products ("Danish Consumer Council. The Nanodatabase." 2018). Amongst synthetic inorganic NP, silver nanoparticles (Ag NP) were the most frequently used nanomaterials in consumer products until 2015 (Vance et al., 2015).

After being released into rivers and lakes (Cleveland et al., 2012), Ag NP can undergo various transformation processes. In the following manuscript, the processes leading to the transformation of NP in the environment without complete loss of the original NP phase are termed "aging processes" (Schaumann et al., 2015). Surface oxidation, coating with natural organic matter (NOM), and cation-induced bridging between NP are aging phenomena which significantly influence the surface properties of NP (Darlington et al., 2009; Nel et al., 2006; Schaumann et al., 2015). Aging in different environmental media therefore has a strong impact on the fate of NP and their colloidal and chemical stability in natural surface water and porous systems. However, the fate of these environmentally modified NP is still underrepresented in the literature (Selck et al., 2016).

Recent studies conducted in complex aqueous systems suggest that unaged Ag NP mainly accumulate in upper sediment layers due to (hetero)aggregation processes and sorption to the solid phase (Coleman et al., 2013; Furtado et al., 2015). Additionally, an accumulation of NP in biofilms is often observed (Ferry et al., 2009; Nevius et al., 2012). Studies investigating the fate of Ag NP in soils have shown that horizontal and vertical translocation is very limited (Schlich et al., 2017) and a remobilization of Ag NP from the solid phase is negligible (Hoppe et al., 2015). Although there are experiments investigating the transport of NP in laboratory sediment columns (such as Zhang and Zhang, 2014 for Ag NP, Lv et al., 2016 for TiO_2, Fang et al., 2016 for CeO_2) and aquifers (Adrian et al., 2018), main retention mechanisms of riverbank filtration systems (such as filtration by biofilms or retention on clay minerals) are not taken into account in most of them. Studies that consider more environmentally relevant conditions suggest that the transport potential of engineered NP in the real environment will be much lower than predicted by laboratory experiments (Emerson et al., 2014). This highlights the need for more complex and realistic outdoor experiments. Therefore, the aim of our study was to investigate the breakthrough and retention of aged Ag NP in riverbank filtration systems and to understand the mechanisms that lead to their remobilization by answering the following questions:

1) *Does the aging of Ag NP in soils or rivers before reaching riverbank filtration systems affect their breakthrough and retention in natural sediments?* Recent studies about NP stability clearly show that a coating with NOM can enhance the colloidal stability of NP (Philippe and Schaumann, 2014). In our study, we focused on aging processes in rivers and soils, leading to the coating of NP with NOM and cation-induced aggregation, two important processes affecting NP stability and fate. Additionally, the dominating process in natural surface waters is heteroaggregation due to the high concentration of natural colloids in environmental systems compared to NP concentrations (Lowry et al., 2012; Praetorius et al., 2014). This might also lead to the co-transport of NP with natural colloids in porous systems (Makselon et al., 2017; Neukum et al., 2014). To account for this process, we used natural, colloid-containing pond water as mobile phase for the transport experiment.
2) *Which mechanisms can induce the remobilization of Ag NP retained in surficial sediment layers?* Long-term mesocosm studies show that the majority of NP in aquatic ecosystems is accumulated in upper soil and sediment layers (i.e. Lowry et al., 2012). Therefore, we hypothesized that a large part of Ag NP would be accumulated in the surficial sediment layers of riverbank filtration systems. In natural systems, these upper sediments are exposed to varying shear forces caused by turbulence in rivers and to changing hydrochemical conditions. While heavy rain falling could dilute river water and reduce ionic strength, flooding might transport a large amount of NOM from floodplain soils into rivers. Both ionic-strength reduction and enhanced NOM concentrations in combination with shear forces have been shown to cause disaggregation of Ag NP homoaggregates (Metreveli et al., 2015). Based on these findings, we aimed at identifying conditions that may cause a remobilization of Ag NP immobilized in the surface sediments of an artificial riverbank filtration system. To detect the main remobilization mechanisms, the properties of remobilized Ag were characterized. This included the differentiation between dissolved and particulate Ag as well the analysis of the aggregation state of Ag NP. Both characteristic are of high importance for a prediction of the fate of remobilized Ag and potential consequences of Ag remobilization.

Our study was undertaken in two parts:

1. The breakthrough and retention of Ag NP, aged in river water, soil extract, and ultrapure water respectively, were studied in a near-natural, water-saturated porous system. The experiments were conducted in an outdoor artificial riverbank filtration system. Compared to laboratory studies as used in the literature (i.e. El Badawy et al., 2013; Liang et al., 2013; Sagee et al., 2012) our system had larger dimensions and was influenced by atmospheric changes. The biological activity was driven by the surrounding pond water conditions.
2. In laboratory batch experiments, we systematically studied the effect of ionic strength, NOM, divalent cations, and mechanical forces on the extent of Ag remobilization. To gain a more mechanistic process

understanding, those experiments were conducted under less realistic conditions, but had a stronger focus on analytics including the use of a high amount of analytical tools. In order to measure dissolved Ag we used a novel interpretation strategy of Graphite Furnace Atomic Absorption Spectrometry (GFAAS) which allowed Ag^+ to be distinguished from Ag NP also when Ag^+ ions were adsorbed to natural colloids or complexed by organic ligands (Feichtmeier and Leopold, 2014). The presence of Ag NP-containing heteroaggregates was tested by combining 1 μm-filtration and Single-Particle Inductively Coupled Plasma-Mass Spectrometry (SP-ICP-MS). With the multiplicity of analyses, we were able to not only identify important remobilization mechanisms, but also characterize the properties of remobilized Ag NP. For some less common analyses, the theoretical background is described in the Supporting Information (SI).

2. Material and methods

2.1. Nanoparticles

We used citrate-stabilized Ag NP that were produced according to the method of Turkevich et al. (1951) modified for Ag which is described in more detail in Klitzke et al. (2015). Transmission electron microscopy (TEM) images can be found in the SI of Metreveli et al. (2015). Particles had a diameter (z-average, determined by dynamic light scattering) of 34 ± 1 nm, a polydispersity index of 0.34 ± 0.01 (both obtained from six replicate measurements) and a ζ-potential of −60.8 ± 0.9 mV (obtained from three replicate measurements).

2.2. Aging procedure

In order to apply Ag NP at more environmentally relevant state, Ag NP were aged in soil extract, and river water (Table S1). Additionally, Ag NP equilibrated in ultrapure water (UPW) were used as a reference for un-aged Ag NP.

Ultrapure water was prepared by an Ultrapure Water System (Evoqua, Water Technologies) and had an electrical conductivity (EC) of 0.055 μS cm^{-1}.

Soil extract was prepared from samples of a Fluvisol taken from a meadow close to the River Rhine near Leimersheim, Germany (GPS: N49°08′13.62″ E008°21′39.6″).

The soil was sieved (2 mm), homogenized and stored field-moist in the refrigerator (4 °C) before use. Soil samples were mixed with water (1:10 mass ratio), shaken on a horizontal shaker (130 rpm, KS501 digital, IKA Labortechnik) for 16 h, and subsequently filtered over a 1.2 μm cellulose nitrate membrane (Type 11303–047 N, Sartorius). To remove suspended soil colloids ($d > 30$ nm, $\rho = 1.2$ g cm^{-3}) the extract was ultracentrifuged (Optima TL, Beckmann) at 156,990 ×g for 1.5 h at 10 °C. The method, adopted by Klitzke et al. (2015), extracts both soluble and colloidal components of the soil. However, in the subsequent centrifugation step we removed colloidal particles in order to study the effect of dissolved soil components only.

River water was sampled from the River Rhine close to the soil-sampling site (GPS: N49°07′26.4″ E008°21′48.3″). Water was filtered (0.1 μm cellulose-nitrate membrane, Whatman) to remove all micron-sized particles.

Soil extract and river water were characterized for pH, dissolved organic carbon (DOC) concentration (TOC-5050 A Shimadzu) and the concentration of main elements (K, Mg, Ca, Na, Al, Fe, and Mn) measured by ICP-optical emission spectrometry (OES) (iCAP 6000, Thermo Scientific, Table S1).

Aging of NP was done by shaking (8 rpm, end-over-end shaker GFL 3040) of a suspension of citrate-stabilized Ag NP (final concentration in the suspension 20 mg L^{-1} Ag NP) in the respective medium for 24 h. Previous experiments showed that this time is sufficient for the sorption process of NOM to NP surfaces to reach equilibrium. The shaking procedure was carried out in ambient light but without any direct sunlight. The ζ-potential of the Ag NP was determined directly after the aging procedure.

2.3. Water-saturated sediment columns

The experimental setting of the artificial riverbank filtration system and the applied analytical methods are summarized in Fig. 1.

The transport experiments were conducted on the German Environment Agency's facility for the simulation of riverbank and slow sand filtration (SIMULAF) located in Berlin, Germany. We used three large-scale, water-saturated sediment columns (diameter 1.13 m, filter area 1 m^2, filter length 1.5 m; followed by a supporting layer of 0.2 m) with a water head of 10 cm, which are embedded in a slow sand filtration pond and are flown through by surrounding pond water extracted on-site from a quaternary aquifer (Fig. 1). This offers the possibility to study a near-natural system where biological processes including biofilm formation take place and natural colloids are present. The columns were filled with coarse-grained medium sand 12 months before the start of the experiment (d_{50}: 0.38 mm, bulk density in the top 10 cm: 1.76 g cm^{-3}; Fe_{tot}: 1.143 ± 0.094 g kg^{-1}, Al_{tot}: 0.869 ± 0.135 g kg^{-1} draining/supporting layer: coarse-grained sand, d_{50}: 1.8 mm; grain size distribution of both sands see Fig. S1). For the experiment, they were fed with a mixture of the pond water (pH 7.0, ionic strength 18.4 mM), and reverse osmosis water (mixing ratio v/v = 1:4). The pH value, EC as well as cation and anion concentrations of this mixture were determined (Tables S2 and S3).

We collected water samples from sampling ports in various depths (30 cm, 50 cm, and 90 cm). The sampling ports consisted of perforated PVC tubes (horizontally installed across the filter area) connected via a stainless steel section to PTFE tubing, leading to a vacuum pump. Additionally, samples were taken at the outflow (i.e. after 1.5 m of sediment passage). Probes were installed at the outflow for the recording of hydrochemical parameters such as EC (Tetracon 325, WTW), pH (SenTix 41, WTW), oxygen content (CellOx 325, WTW), and redox potential (SenTix ORP, WTW, values were corrected for the standard potential of the redox probe relative to the hydrogen normal electrode at 20 °C, i.e. +211 mV). In addition, EC was monitored in the supernatant.

2.4. Design of near-natural column experiments

A filter velocity of 0.2 m day^{-1} (pore velocity 0.5 m day^{-1}) was adjusted and kept constant throughout the entire experiment. This filter velocity was selected to allow for diffusive transport and to minimize any potential shear forces in the flow system. Tracer experiments were conducted prior to NP application. As tracer 400 mL of a NaCl solution (25 wt%), diluted up to 5 L with infiltrating water, was added to the supernatant as pulsed application. For the detection of the tracer the EC was recorded in the water head above the column, in the three sampling depths, and at the outflow. The tracer experiments were conducted 15 days prior to the start of NP application to ensure that added NaCl had completely left the system to avoid any interference with the NP due to increasing ionic strength.

Prior to the start of NP injection, blank samples of the water head, as well as from the individual depths and the outflow were taken. In each of the three columns, a suspension of one kind of the differently aged NP was added to the supernatant as pulsed application to reach a final concentration of 1 mg L^{-1} Ag in the supernatant. This is higher than environmentally relevant concentrations but high enough to still analytically quantify the particles. The infiltrating volume of the spiked supernatant amounted to 100 L (i.e. 0.2 pore volumes of the entire column volume). After gentle stirring of the supernatant of the column, water samples were taken to determine initial Ag NP concentrations (5 replicates) in the water head and to characterize Ag NP size using Hydrodynamic Chromatography coupled with an Inductively Coupled Plasma-Mass Spectrometer (HDC-ICP-MS, XSeries 2, Thermo Scientific; for detailed information see SI). Water samples at the outflow and in the

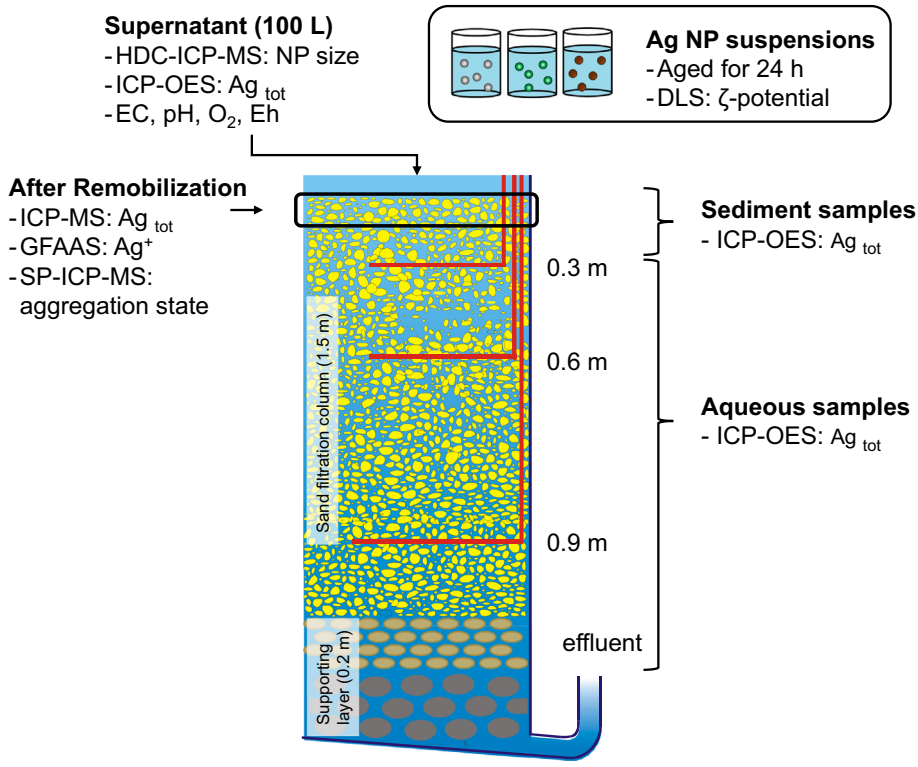

Fig. 1. Cross section of water-saturated sediment columns. The horizontal tube of the sampling ports in 0.3, 0.5 and 0.9 m depth is composed of PVC, the vertical tube of stainless steel. At the top end of the stainless steel tubes, PTFE tubes lead to a vacuum pump. Explanations surrounding the graph describe the main analytical techniques used and parameters measured during this study, including total silver (Ag_{tot}), dynamic light scattering (DLS), electrical conductivity (EC) and redox potential (Eh).

various depths were taken over the course of 19 weeks (29th of April 2014 until 13th of September 2014). For analysis, a sample volume of 10 mL was transferred into a crucible and dried at 40 °C until complete evaporation of the water. To digest Ag NP, concentrated nitric acid was added. The acid was evaporated to a remainder of approximately 0.5 mL and subsequently diluted with UPW to a volume of 25 mL. The recovery of this method was determined to be 95 ± 10% (Table S4 in SI).

To quantify concentrations of Ag NP retained in the column, sediment samples in 0–10, 10–20, and 20–30 cm depth were taken at three different "zones" to account for any heterogeneity in the system at the end of the experiment. At each zone, four to six samples were taken. The samples of each depth were homogenized to one sample and stored at 4 °C. Sediment samples were dried for 24 h at 105 °C, prior to digestion. Concentrations of Ag were determined following nitric acid (HNO_3, 69%) digestion in closed vessels at 185 °C for 8 h.

The total Ag content in aqueous and sediment samples was analyzed using ICP-OES (iCAP 6000, Thermo Scientific, λ = 328.0 nm).

Recoveries (R) of Ag in the sand were calculated according to Eq. (1):

$$R = \frac{(c_{sand1} + c_{sand2} + c_{sand3}) * d_{bulk} * V_{sand}}{c_{water} * V_{water}} \quad (1)$$

with c_{sand1} being Ag concentration in the sand (depth 0–10 cm), c_{sand2} being Ag concentration in the sand (depth 10–20 cm), c_{sand3} being Ag concentration in the sand (depth 20–30 cm) all in mg kg^{-1}; d_{bulk} being the bulk density of the sand [kg L^{-1}]; V_{sand} being the volume of the sand in the respective depth [L]; c_{water} being the initial Ag concentration in the supernatant [mg L^{-1}]; V_{water} being the water volume of the supernatant [L].

2.5. Zeta potential and size of nanoparticles

Nanoparticles used for the column experiments were characterized prior to and after the aging procedure regarding their size and ζ-potential.

The ζ-potential of aged NP stock suspensions (c_{Ag} = 20 mg L^{-1}) was analyzed using a Zetasizer 2000 photon correlation spectrometer (Malvern instruments) and calculated based on the electrophoretic mobility of the NP (using the Helmholtz-Smoluchowsky equation).

Particle sizes in the column supernatant were determined by HDC-ICP-MS (SI, Section 2.3) as the presence of natural colloids would interfere with measurements of Ag NP by dynamic light scattering (DLS).

2.6. Remobilization experiments

Batch experiments with the sediment samples of the first 10 cm of the three columns, each containing NP with a different aging history, were conducted to understand the reversibility of NP attachment. We investigated the amount of potentially remobilizable Ag as well as the characteristics of remobilized Ag to gain information on remobilization mechanisms. Silver concentrations in these sediments accumulated during column experiments were 0.48, 0.70 and 0.31 mg kg^{-1} for UPW-, river water- and soil-aged Ag NP. The sediment samples were subjected to a remobilization procedure with varying mechanical forces as well as hydrochemical conditions (Table 1). Batch experiments were conducted in triplicates.

The soil extract was obtained from the floodplain soil of the River Rhine using the same procedure as for aging experiments (see Section 2.3). The Suwannee River-NOM (SR-NOM) powder was obtained from the International Humic Substances Society (IHSS). The preparation of the stock solution is described in the SI.

NH_4NO_3 solution can be used for the determination of the cation exchange capacity of soils (DIN ISO 13536) due to the strong sorption of NH_4^+ to soil surfaces, thereby exchanging cations originally bound to surfaces. NH_3 also forms stable complexes with Ag^+ ions which promotes the dissolution of Ag. Therefore, NH_4NO_3 solution was used as remobilizing medium before GFAAS measurements to investigate the potential of Ag^+ ion release of retained Ag NP.

Table 1
Remobilization procedure which includes applying mechanical forces and changing hydrochemical conditions.

Mechanical forces		Hydrochemical conditions	
Force	Concept	Remobilization medium	Concept
Manual shaking, 5 s	Weak forces	UPW	Ionic strength reduction
Horizontal shaking, 24 h, 130 rpm	Medium forces	Soil extract (DOC 5.5 mg L^{-1})	Presence of NOM and Ca^{2+}
Ultrasonic bath[a] (USB), 5 min, 35 kHz	Strongest forces (operationally defined)	SR-NOM (30 mg L^{-1})	Presence of Model-NOM
		NH_4NO_3 (0.1 M)	Potential of Ag^+ release

[a] USB: 2 × 240 W, Bandelin Sonorex RK 255H.

The chemical composition of soil extract and SR-NOM solution are summarized in Table S5.

Sediments were mixed with each of the four types of remobilizing media (Table 1) in a ratio of 1:5 (10 g sediment + 50 mL of remobilizing medium). The pH of the solutions was measured and adjusted with dilute NaOH to 8 ± 1 if necessary (pH-Meter 761 Calimatic, Knick, Th. Karow GmbH). In this pH range Ag NP have a negative ζ-potential. After the remobilization procedure the pH was checked again.

At the end of the remobilization procedure sediments were down-centrifuged using a cut-off diameter of 3 μm (corresponding to 1.25 μm for Ag NP) which was smaller than the mean size of the sand particles in the columns (7.3 ×*g* calculated for spherical SiO_2 particles, 5 min). The supernatant containing remobilized Ag was stored in amber bottles at 4 °C until analyses. The samples were analyzed for total Ag and Al by ICP-MS following acid microwave digestion (Section 2.7.1).

Particle size and morphology as well as elemental composition were determined by Scanning Electron Microscopy (SEM) coupled with an Energy Dispersive X-Ray (EDX) analysis (Section 2.7.4).

A combined approach of filtration and SP-ICP-MS was used in order to investigate the aggregation state of remobilized Ag NP (Section 2.7.3). Differentiation of particulate and dissolved Ag was done using GFAAS (Section 2.7.2).

2.7. Analyses of remobilization samples

2.7.1. Determination of total Ag and Al in remobilization experiments

In order to determine the concentration of total Ag remobilized from sediment samples, the supernatants obtained after centrifugation were digested by acid microwave digestion (MARS Xpress, CEM, Matthews, USA). For the digestion, a mixture of nitric acid (HNO_3, ≥65%, p.a., ISO, ROTIPURAN, Carl Roth, Karlsruhe, Germany) and hydrochloric acid (HCl, 35%, ROTIPURAN Supra, Carl Roth, Karlsruhe, Germany) was prepared at a volume ratio of 1:1. In Teflon digestion vessels 10 mL sample were mixed with 4 mL acid mixture. In order to check the background concentration of analyzed elements, 10 mL UPW were also mixed with 4 mL acid mixture. The digestion was performed using a two-step temperature program (temperature ramp of 30 min from room temperature to 95 °C and subsequent 30 min irradiation at a constant temperature of 95 °C at 800 W). After cooling, the digested samples were diluted with 28 mL UPW and analyzed by ICP-MS (XSeries 2, Thermo Scientific). The detector signal drift was corrected by an internal standard Rh (Rhodium internal ICP-MS standard Fluka, Sigma-Aldrich, St. Louis, USA). In order to observe a trend in the remobilization of natural inorganic colloids, the concentration of Al was also measured in the digested samples.

For quality control of the ICP-MS analysis we also measured the reference materials TMDA-51.5 and TMDA-54.5 (both from LGC Standards, Wesel, Germany) containing Ag and Al. The determined concentrations of Ag and Al in both reference materials were in the range of the nominal values given by the provider showing high accuracy of the ICP-MS measurements (Fig. S2). The limit of detection (LOD) and limit of quantification (LOQ) were 0.05–0.2 μg L^{-1} and 0.14–0.5 μg L^{-1} for Ag and 1–5 μg L^{-1} and 3–11 μg L^{-1} for Al, respectively.

2.7.2. Graphite furnace atomic absorption spectroscopy

Graphite furnace AAS measurements were conducted from selected samples of the remobilization experiment treated with ultrasonic bath (USB) in UPW, soil extract, and NH_4NO_3 for the three types of differently aged Ag NP. Measurements were performed using a high-resolution continuum source atomic absorption spectrometer contraAA 600 (Analytik Jena AG, Germany).

For data interpretation, the atomization delay (t_{ad}) was determined as first described by Feichtmeier and Leopold (2014). Briefly, t_{ad} is the time from the starting point of the atomization process until the maximum of the absorbance signal. The maximum was determined by fitting a polynomial or Gaussian function on the absorbance signal, depending on the signal shape. Obtained t_{ad} values indicate the presence of Ag^+ and/or can be used to determine Ag NP size after calibration of the method (for details see SI, Section 1.1, Theoretical considerations). To prove the applicability of this method to the samples of the remobilization experiment, the matrices of those samples were spiked with Ag^+ and Ag NP and GFAAS measurements were conducted. Statistically significant differences of t_{ad} values were obtained when comparing t_{ad} of Ag^+ ions with 5 nm Ag NP ($t_{ad}(Ag^+) = 1.338 \pm 0.009$ s; t_{ad}(5-nm-AgNP) = 2.201 ± 0.016 s; n = 4). Hence, an indication for Ag^+ ions was given by an early peak or shoulder at $t_{ad} = 1.34 \pm 0.01$ s, which was clearly detectable in a concentration range from 5 to 30 μg L^{-1}. Precision of t_{ad} determination calculated as standard deviation (SD) with n ≥ 4 was found to range between 0.01 and 0.08 s for replicate measurements. Day to day variation of t_{ad} - including usage of different graphite platforms - was in a range of 0.15 s. Moreover, no matrix effects on t_{ad} were observed in the media studied here, independent on whether Ag^+, Ag NP or a mixture were present (Fig. S4). The LOD of Ag with this method was 1.23 μg L^{-1}.

Size calibration was performed using commercially available Ag NP suspensions with defined particle sizes as standard solutions in a size range from 5 to 200 nm, diluted to the desired concentration. With the found t_{ad}-size-correlation, NP size given as modal diameter (most commonly found size distribution) was calculated. The resulting calibration function ($t_{ad} = 0.144 \ln(\text{NP size [nm]}) + 1.963$; $R^2 = 0.9902$; N = 32) is shown in Fig. S3 and revealed high precision. The lower size limit as derived from this calibration was found to be as small as 1.1 nm. Hence, the minimum Ag NP size that can be distinguished from Ag^+ ions using this size calibration is 1.1 nm. Furthermore, no effect on t_{ad} was observed when silver concentrations varied in a range between 2.5 and 40 μg L^{-1}.

Further experimental details on sample preparation, calibration and instrumental parameters of GFAAS measurements can be found in the SI (Section 2.3).

2.7.3. Single Particle-Inductively Coupled Plasma-Mass Spectrometry

Analyses by SP-ICP-MS (XSeries 2, Thermo Scientific) were performed in order to investigate the size range of Ag-containing aggregates (smaller or larger than 1 μm) as well as the number of Ag NP per aggregate. Hereby, the presence or absence of heteroaggregates of Ag with natural colloids was detected. Therefore, samples were measured by SP-ICP-MS before as well as after filtration (PTFE, 1 μm, Puradisc 25 TF, Whatman, GE Healthcare Life Science).

The samples were diluted 1:10 with UPW prior to filtration and the measurements to minimize particle coincidence. A dwell time of 5 ms was used for monitoring ^{107}Ag. The particle size detection limit of the instrument was approximately 30 nm for Ag NP. Citrate and tannic acid capped Ag NP standards (Nanocomposix) of a size of 40, 80, and 100 nm were measured prior to and after sample measurement for size calibration as well as for monitoring the sensitivity drift which was found to be negligible. Detailed characterization of these standards can be found elsewhere (Philippe et al., 2014).

The data of SP-ICP-MS were analyzed using a self-programmed R-Script which is described in detail in the SI. In short, the background signal was determined and spike signal intensities were corrected for the background value. Subsequently, the average number of Ag NP per aggregate ($\overline{N}$) and the portion of linear homoaggregates >1 μm ($W_{linear>1}$) of total Ag-containing aggregates were calculated for each sample (Eqs. (2)–(4)). For all calculations, we assumed that the size of the primary particles was not significantly changed in the samples e.g. through dissolution processes.

$$\overline{N} = \frac{\bar{I}}{I_{prim}} \tag{2}$$

where $\bar{I}$ is the average spike signal intensity in the sample and I_{prim} is the average signal intensity of primary Ag NP measured separately.

$$d_{linear} = \frac{I_x}{I_{prim}} * d_{prim} \tag{3}$$

$$W_{linear} = \frac{N_{linear>1}}{N_{tot}} \tag{4}$$

with d_{linear} being the length of a homoaggregate assumed to be linear calculated for each spike, I_x each spike signal intensity and d_{prim} the average size of primary Ag NP, $N_{linear>1}$ the number of linear homoaggregates >1 μm and N_{tot} the total number of peaks per sample. With this calculation, the portion of homoaggregates will most probably be overestimated as the linear shape is unlikely. Therefore, the portion of homoaggregates >1 μm might be smaller than calculated.

The maximal portion of homoaggregates larger than 1 μm was compared to the portion of peaks actually removed by filtration ($W_{removed}$: obtained by subtraction of spike numbers in filtered samples from numbers in unfiltered samples). The difference between both portions was assumed to be caused by the presence of heteroaggregates of Ag NP and natural colloids (for more detailed information see Section 1.2 in the SI). Therefore, the portion of Ag-containing heteroaggregates >1 μm (W_{hetero}) was calculated using Eq. (5).

$$W_{hetero} = W_{removed} - W_{linear} \tag{5}$$

As filtration is often biased due to the possibility for filter clogging (Zirkler et al., 2012), we calculated the recovery of the filtration step by filtering a sample of primary Ag NP (34 nm) with a concentration comparable to remobilization samples, subsequently measuring the Ag concentration by ICP-MS. This recovery of 66% was taken into account in the calculation of particle numbers by multiplying the calculated values with 1.5.

2.7.4. Scanning Electron Microscopy

Three samples of the remobilization experiment were selected for SEM/EDX analysis (24 h shaking, 130 rpm, aged in UPW, river water and soil extract, and remobilized in UPW). The samples were air-dried on a silicon waver. Analyses were conducted at the Center for Electron Microscopy (ZELMI) of the TU Berlin with an SEM (Zeiss DSM 982 Gemini) coupled with an EDX detector (EDX; EDAX, software 'TEAM', detector 'Apollo' — acquisition parameters of the beam: accelerating voltage: 15 and 20 kV). Due to low Ag concentrations, no quantitative information was gained, but shape and size of the Ag NP as well as the elemental composition in the area of the particle were investigated.

Additionally, a sample of the surficial sediment of two of the columns was studied by SEM to demonstrate the presence of biofilm-forming organisms in the system using measurement conditions as described above. The sediments were taken three years after the transport experiment, but columns had been fed with pond water before and after the experiment, continuously. Although the ecological community might have changed during this time, evidence for the presence or absence of organisms can be provided.

3. Results

3.1. Nanoparticle properties in the column supernatant

The ζ-potentials of Ag NP aged in both soil extract (−26.8 ± 1.4 mV; pH 8.3, EC 347 μS cm^{-1}) and river water (−24.8 ± 0.7 mV; pH 8.2, EC 462 μS cm^{-1}) were similar but less negative than the value of the Ag NP aged in UPW (−42.0 ± 1.2 mV; pH 9.0, EC 324 μS cm^{-1}).

In HDC-ICP-MS measurements, samples collected from the supernatant showed that Ag NP aggregated after addition to the supernatant of the column. Largest aggregate sizes were measured for Ag NP aged in river water (406 ± 31 nm) and smallest aggregate sizes for Ag NP aged in UPW (244 ± 15 nm), whereas soil-aged Ag NP aggregates had an intermediate size (317 ± 10 nm). In all cases the aggregate size in the supernatant was an order of magnitude larger than the primary particle size of original, unaged Ag NP (34 ± 1 nm).

3.2. Characteristics of the columns

Values of pH and EC in the column supernatant did not differ significantly before and after NP addition (Table S2). The tracer broke through after one pore volume which means on average after 46.5 h (Fig. S5). Hydrochemical parameters (Figs. S6–S9) measured at the column outflow showed pH values of 7.9 ± 0.3, mostly oxic conditions and EC between 200 and 400 μS cm^{-1} that was reduced to values below 150 μS cm^{-1} by several rain events during the experiment.

The SEM picture of surficial sediments of two columns shows a high number of diatoms distributed over the entire range of the analyzed sediment sample (Fig. S15). This highlights the presence of biofilm forming organisms in the near-natural sediment system.

3.3. Silver breakthrough and retention

In general, we observed low and irregular Ag breakthrough in all depths of the column that appeared only in erratic events leading to single peaks in the graphs instead of the expected breakthrough curve (Figs. S10–S12). The most frequent breakthrough events were detected in 30 cm depth (Fig. 2). A complete mass balance was not obtained from our results as the sampling frequency during breakthrough was not high enough due to logistic and time constraints. A correlation between NP breakthrough and the intensity of precipitation events, i.e. mobilization of particles due to dilution of the feeding water, was not detected.

Silver contents in the sand were largest in a depth of 0–10 cm, and significant amounts were also measured between 10 and 20 cm. However, no Ag was detected below 20 cm (Fig. 3). The data showed a high variability between different sample locations of the same depth. Measured Ag contents in the sediments indicated lowest retention for soil-aged Ag NP (recovery of 54 ± 24% in sand) and strongest retention for river water- and UPW-aged Ag NP (recoveries of 132 ± 25% and 116 ± 20% in sand, respectively). A retention of only 54% of soil-aged Ag NP indicates that those NP were transported below a depth of 30 cm even though a breakthrough was not proven by Ag concentrations in the aqueous samples. Silver NP aged in river water and UPW, instead, were almost completely retained in the upper 20 cm of the sediments.

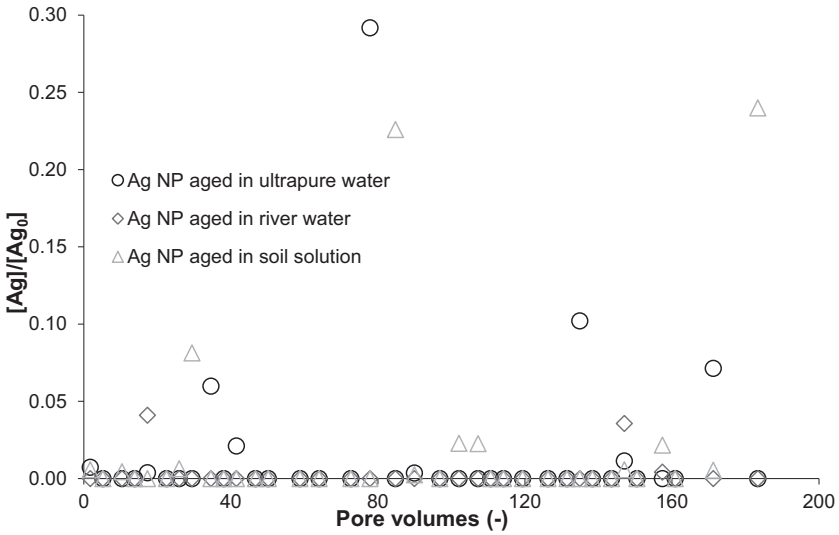

Fig. 2. Breakthrough of the differently aged Ag NP in 30 cm depth as a function of pore volumes. Initial Ag concentration: $c_0 = 0.96$ mg L^{-1} (ultrapure water); $c_0 = 1.02$ mg L^{-1} (river water); $c_0 = 1.02$ mg L^{-1} (soil extract).

3.4. Remobilization of Ag NP from sediments

3.4.1. Amount of remobilized Ag

Between 8 and 50% of Ag was potentially remobilizable by mechanical forces and hydrochemical changes (Fig. 4). Increasing mechanical forces led to an enhanced release of Ag from the sediments. A difference between treatments was assumed when the standard deviation of replications was smaller than the difference between treatments (i.e. when the standard deviations of treatments were not overlapping). Due to the low number of replicates further statistical evaluation was not undertaken.

A short manual shaking procedure in the different remobilizing media introducing only weak and short pulse shear forces, remobilized 8–15% of Ag from sediments, most likely mainly by changing hydrochemical conditions, i.e. the reduction of ionic strength and the input of NOM. An effect of the aging history was not visible in the case of soil extract and SR-NOM as remobilizing medium. In both cases, 8–12% of Ag was remobilized. A reduction in ionic strength (i.e. the remobilization in UPW) led to a slightly higher remobilization of up to 15% of retained Ag for NP that had been aged in solutions with higher ionic strength and NOM content (i.e. Ag NP aged in river water and soil extract) compared to particles aged in UPW.

When medium mechanical forces acted on the sediments in the form of horizontal shaking for an extended time period (i.e. 24 h), more Ag was remobilized (18–30%), irrespective of the hydrochemical conditions of the remobilizing medium. However, the degree of remobilization differed depending on the aging history of Ag NP: soil-aged Ag NP showed the highest remobilization while Ag from UPW-aged Ag NP was remobilized in lowest amounts.

Remobilization in UPW and soil extract at strongest mechanical forces (i.e. USB treatment) detached on average one third of retained Ag irrespective of NP aging history. While the release of Ag slightly, but not significantly increased in the case of UPW- and river water-aged Ag NP compared to 24 h shaking, soil-aged Ag NP did not show stronger remobilization after ultrasonic treatment despite of the increased mechanical forces.

The presence of SR-NOM during USB treatment led to a remobilization of up to 50% of retained Ag NP and a significantly increased Ag

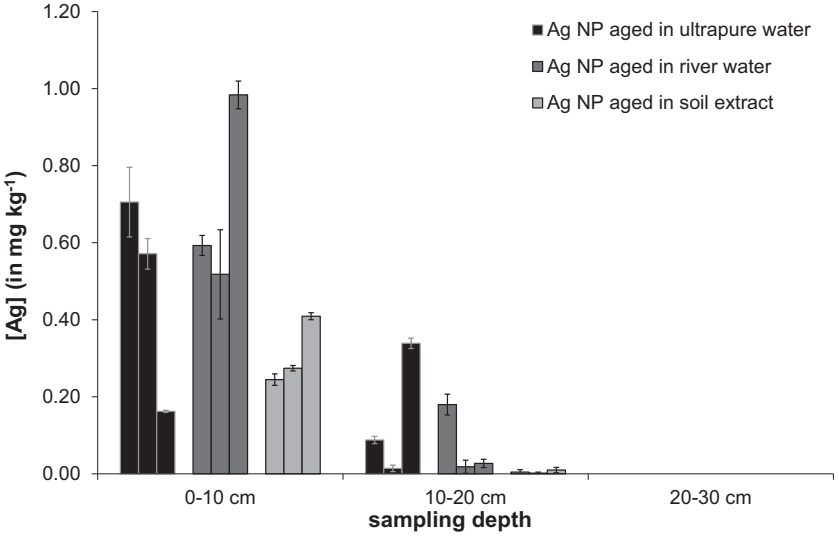

Fig. 3. Ag concentration in sand at various depths (0–10, 10–20, 20–30 cm) and for differently aged Ag NP. The same colors for each depth depict the values for different sampling locations in the column. Error bars depict the standard deviations from three replicates.

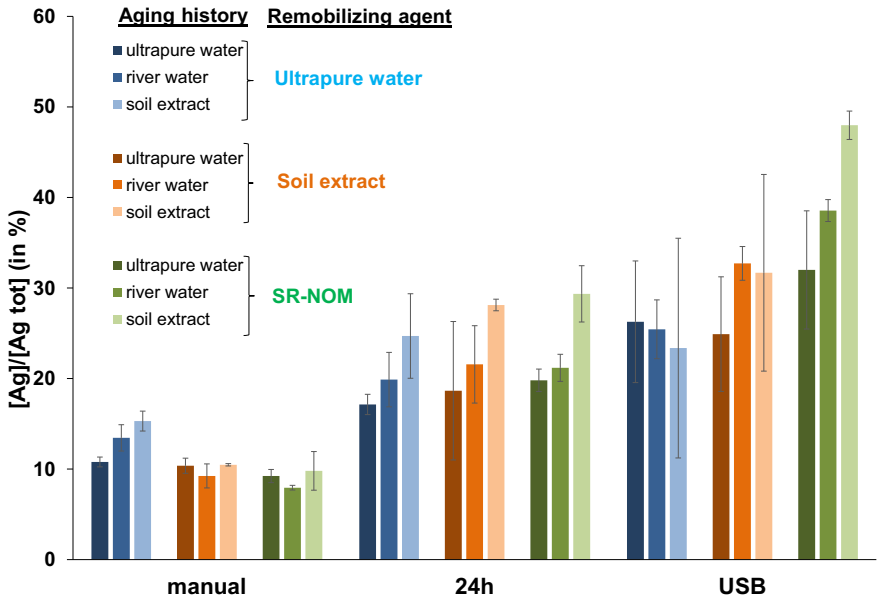

Fig. 4. Portion of Ag remobilized by UPW (blue bars), soil extract (orange bars), and SR-NOM (green bars) from sediments applied in the riverbank filtration experiments with differently aged Ag NP. The portion of remobilized Ag is normalized to Ag concentrations of the respective sediments (different color scales show different aging history, bars reflect the median, arrow bars depict the standard deviation from 3 replicates).

remobilization at strongest mechanical forces compared to horizontal shaking. Compared to remobilization in UPW and soil extract an increased Ag release of around 25% for UPW-aged, 33% for river water-aged and even 74% for soil-aged Ag NP was observed.

3.4.2. Characteristics of remobilized Ag

3.4.2.1. Discrimination between Ag NP and Ag^+ ions. Graphite furnace-AAS was applied to selected samples of the remobilization experiment to gain information about the size of Ag NP as well as the appearance of Ag^+ ions. For the latter goal, NH_4NO_3 was used as remobilizing medium to measure the potential for Ag^+ release from retained Ag NP or sediment surfaces.

Largest particle sizes were measured for Ag NP aged in river water compared to UPW- and soil-aged Ag NP in all remobilizing media (Table 2). This is in accordance with HDC-ICP-MS measurements of Ag NP after addition to the column supernatant (3.1). Nevertheless, particle sizes of remobilization cannot be compared directly with the ones in the column experiment as mechanical forces of the remobilization procedure are expected to have an influence.

Additionally, the remobilizing medium had a strong influence on the size of remobilized Ag NP. While remobilization in NH_4NO_3 solution and UPW preserved the primary particle size range of Ag NP (12–40 nm), Ag NP remobilized in soil extract formed larger aggregates (188–220 nm). The aging of Ag NP and their residence in the sediment column enhanced NP stability as spiking of NH_4NO_3 solution with primary ('unaged') Ag NP (Table 2, sample 1) led to a larger size of Ag NP compared to differently aged Ag NP remobilized in NH_4NO_3 (Table 2, sample 7–9). This illustrates that unaged Ag NP were less stable against ionic strength induced aggregation than aged Ag NP.

The GFAAS is a promising method for distinguishing NP from ions in samples containing larger particles and organic molecules where filtration would be biased by removal of adsorbed or complexed Ag^+ that would not pass the filter. Preliminary experiments of GFAAS suggested that this method cannot distinguish between free and complexed or adsorbed Ag^+ (see Theoretical background in the SI).

Samples from remobilization experiments using NH_4NO_3 solution as remobilizing medium exhibited peaks at t_{ad} = 1.6–1.8 s which corresponds to Ag^+ ions (Fig. 5, sample 8) whereas samples with soil extract or UPW did not show a clear indication for the presence of Ag^+ (Fig. 5, sample 6 and 12). This suggests that the main Ag species after remobilization experiments was particulate Ag. Only in the presence of NH_4NO_3 the complexation of Ag^+ with NH_3 most likely enhanced Ag dissolution.

Table 2
Atomization delay (t_{ad}) and average size of Ag NP in selected samples of remobilization experiment with USB treatment measured by GFAAS and calculated from calibration curve (Fig. S3), 'Unaged' samples contain the respective remobilizing medium and primary Ag NP (30 nm) added shortly before analysis. Grey lines mark the samples depicted in Fig. 5.

	Aging history[a]	Remobilizing medium	t_{ad} [s]	NP size [nm]
1	Unaged	NH_4NO_3	2.66 ± 0.01	**123 ± 9**
2	Unaged	UPW	2.43 ± 0.02	**26 ± 4**
3	Unaged	Soil extract	2.71 ± 0.02	**172 ± 25**
4	UPW	UPW	2.34 ± 0.08	**15 ± 7**
5	RW	UPW	2.42 ± 0.02	**25 ± 4**
6	SE	UPW	2.31 ± 0.01	**12 ± 1**
7	UPW	NH_4NO_3	2.44 ± 0.03	**29 ± 5**
8	RW	NH_4NO_3	2.49 ± 0.04	**40 ± 11**
9	SE	NH_4NO_3	2.39 ± 0.03	**20 ± 5**
10	UPW	Soil extract	2.72 ± 0.02	**188 ± 21**
11	RW	Soil extract	2.75 ± 0.02	**220 ± 37**
12	SE	Soil extract	2.72 ± 0.06	**194 ± 74**

[a]RW: river water; SE: soil extract.

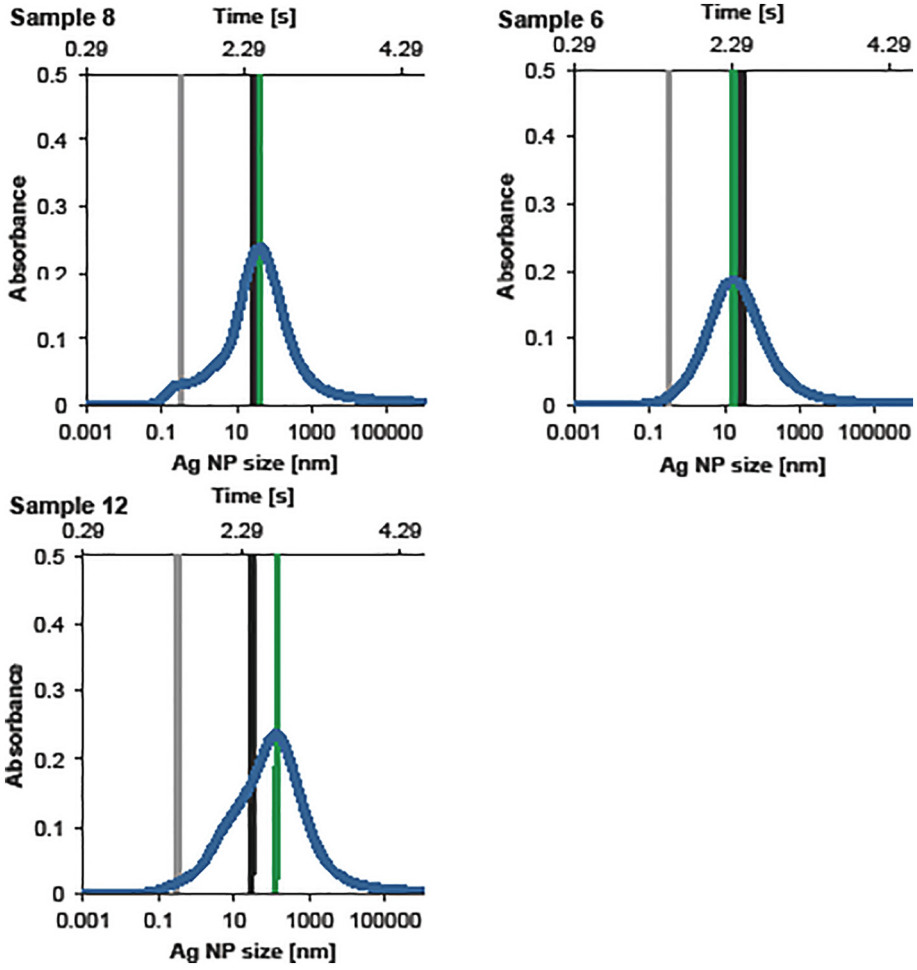

Fig. 5. GFAAS absorbance signal (blue) of the samples 8 (remobilization in NH_4NO_3), 6 (remobilization in UPW) and 12 (remobilization in soil extract). The grey line corresponds to free silver ions, the black line shows the size of initial unaged Ag NP (30 nm), and the green line represents the mode of particle size distribution of the respective sample.

Dissolved Ag was also found in soil extract that was spiked with primary Ag NP but not in samples where soil extract was used as remobilizing medium (compare sample 12 and 3 in Figs. 5 and S13, respectively). This suggests that soil extract increased the dissolution of Ag NP. But when Ag NP had been aged and exposed to natural surface water in the column experiments they seemed to be stabilized against dissolution during remobilization experiments.

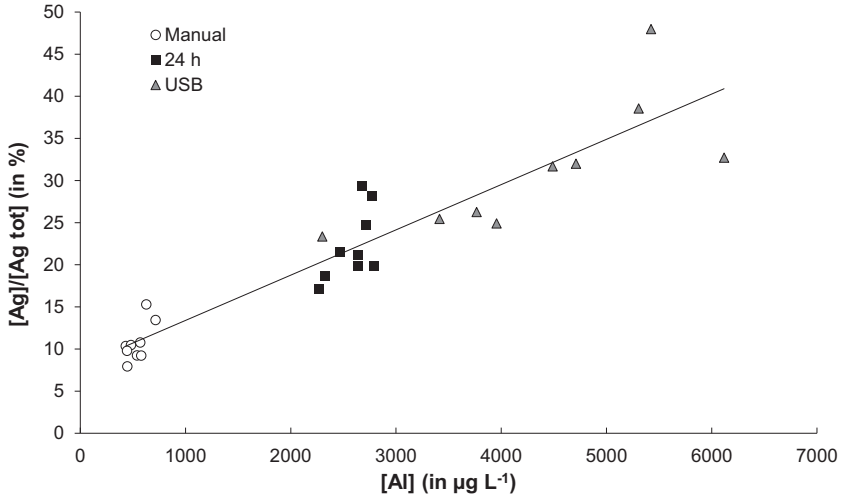

Fig. 6. Correlation of remobilized Al and Ag concentrations measured in the corresponding samples from remobilization experiments. The concentration of remobilized Ag is normalized to the total Ag concentration of the respective sediment. Circles represent data from manually shaken samples, squares exhibit data from 24 h shaken samples and triangles represent data from samples treated with USB. The line corresponds to a linear regression with $R^2 = 0.8614$.

3.4.2.2. Aggregation and transformation state of remobilized Ag NP. In order to investigate the potential correlation between remobilized Ag and inorganic colloids released from sediments in the samples of remobilization experiments the concentration of Al was measured as a tracer for natural inorganic colloids such as clay particles. With increasing Ag concentration, the Al concentration also increased (Fig. 6) indicating a co-mobilization of Ag NP with Al-containing natural colloids. The remobilization of Al-containing colloids increased also with increasing mechanical forces as shown by a grouping of the data points treated with similar mechanical forces.

As a second approach to characterize Ag NP aggregation state, SP-ICP-MS combined with 1 μm-filtration of selected samples containing remobilized Ag was used. Thereby, the size range of the remobilized aggregates or particles and the amount of Ag-containing heteroaggregates were investigated. The average spike signal intensities of unfiltered samples indicate that particles contained between one and two primary Ag NP on average (Table 3). Most Ag-containing particles should therefore be smaller than the cut-off of the used filter (1 μm) if they were primary particles or homoaggregates. The recovery rate of the filtration step proved that 66% of primary Ag NP passed the filter (Section 2.7.3); hence we corrected our calculations by this factor. From signal intensities, we calculated the maximal possible size of homoaggregates for a given number of primary particles by assuming their shape to be linear. The linear geometry is highly unlikely as most homoaggregates should be more compact with fractal dimensions of 1.7–2.5 (Meakin, 1988). Therefore, the maximal possible length for a homoaggregate proposed here was a quite rigid criterion for distinguishing hetero- from homoaggregates. Still, those calculations suggest that most Ag-containing aggregates ($99.7 \pm 0.3\%$) should pass the filter. In contrast, filtration of the samples led to a low count rate (average number of spikes) of only 7–26% of unfiltered samples in SP-ICP-MS measurements (exemplary graphs are shown in Section 3 of SI). Hence, only a small amount of Ag-containing particles or aggregates smaller than 1 μm was present in the samples (Table 3). This indicates that the majority (at least 74–93%) of the detected particles were heteroaggregates larger than 1 μm. As the recovery of the filtration step was included in this calculation, filter clogging cannot be the process responsible for particle exclusion. Although we cannot exclude that some smaller homoaggregates of Ag NP might have co-precipitated during the filtration step, the high recovery of single Ag NP during filtration showed that the interaction between NP and the filter material was low.

During SEM measurements only few Ag NP were found due to the low Ag concentrations in the range of μg L^{-1}.Those had a size of 120 nm and EDX spectra showed the coexistence of Ag with S and Fe (data not shown). Sulfur was not present at other Ag-free spots of the sample which suggests a correlation with Ag. The measurements were not interpreted quantitatively due to the low sample concentration but showed that at least a part of Ag NP was sulfidized.

4. Discussion

4.1. Transformation reactions of Ag NP in aging media and column water

The aging of citrate-stabilized Ag NP in three different media (i.e. UPW, river water, and soil extract) led to varying surface properties of the NP. Compared to Ag NP aged in UPW, less negative ζ-potentials were observed for river water- and soil-aged Ag NP which may be attributed to charge neutralization caused by cations such as Ca in the respective media since Ca was a major element present in soil extract and river water (Table S1). This is in line with previous studies showing the predominant role of Ca ions for charge neutralization of citrate-stabilized Ag NP in soil extract (Klitzke et al., 2015) and river water (Metreveli et al., 2015).

In the column supernatant, the differently aged Ag NP were subjected to diluted, natural pond water which induced particle aggregation, most likely due to the presence of Ca (1.2 mM). Despite their similar ζ-potentials, soil-aged and river water-aged Ag NP differed significantly in aggregate size once in the column supernatant. The smaller aggregate size of soil-aged Ag NP may be attributed to the larger DOC concentration in the soil extract, forming a stabilizing coating layer on the surface of Ag NP (Klitzke et al., 2015). The larger aggregate size of the Ag NP aged in river water can be explained by the elevated Ca concentration and the relatively low DOC concentration in the aging medium facilitating the destabilization of Ag NP. UPW-aged Ag NP had smallest aggregate sizes as no Ca was present during aging and therefore the ζ-potential was strongly negative.

4.2. Retention mechanisms in riverbank filtration systems

Our study showed that the breakthrough of Ag NP in the sediments of an artificial riverbank filtration system was irregular and very erratic. This was similar for all differently aged Ag NP. Large Ag contents were found in the sediments of the upper 10 cm of the columns which was in line with the finding that Ag NP aged in river water and UPW were almost completely retained in the column. Nevertheless, only $54 \pm 24\%$ recovery of soil-aged NP in the upper 30 cm of the sediments was calculated. Thus, the aging of Ag NP in soil extract seems to have led

Table 3
Results of SP-ICP-MS measurements of selected samples. The number of particles per aggregate was calculated from sample spike intensity divided by the average spike intensity of primary Ag NP. The minimal portion of heteroaggregates was determined based on the amount of spikes removed by filtration minus the number of homoaggregates being large enough to be filtered out. The latter value is estimated based on the spike intensities assuming a linear geometry for the aggregates (see SI, Section 1.2 for more details).

Sample (aging/remobilization medium/mech. force)[b]	Average number of primary NP per particle ($\overline{N}$)	Portion of spike counts after filtration ($W_{removed}$) [%] [1]	Portion of linear homoaggregates > 1 μm (W_{linear}) [%][a]	Minimal portion of heteroaggregates (W_{hetero}) [%][a]
SE/UPW/man.	1.47	9.56	1.20	89.24
SE/UPW/man.	1.43	13.49	0.30	86.21
SE/UPW/man.	1.41	21.23	0.32	78.45
SE/UPW/24 h	1.49	16.23	0.30	83.47
SE/UPW/24 h	1.87	9.91	0.50	89.59
SE/UPW/24 h	1.44	25.24	0.35	74.41
UPW/NH_4NO_3/USB	2.05	15.40	0.18	84.42
RW/NH_4NO_3/USB	1.99	16.73	0.36	82.91
SE/NH_4NO_3/USB	1.80	15.53	0.26	84.21
UPW/UPW/24 h	2.00	13.34	0.12	86.54
SE/UPW/24 h	2.19	13.58	0.30	86.12
SE/SE/man.	1.32	18.75	0.24	81.01
SE/SE/man.	1.40	16.28	0.32	83.40
SE/SE/man.	1.37	25.74	0.06	74.20
SE/SE/USB	1.93	8.94	0.24	90.82
SE/SE/USB	2.05	7.04	0.26	92.70

[a] Corrected by recovery of filtration (66%).
[b] SE: soil extract; UPW: ultrapure water; RW: river water.

to a higher mobility of the soil-aged NP in the columns. Still, those Ag NP were also accumulated in the upper 10 cm of the column. The different retention behavior cannot be correlated with the size of differently aged Ag NP as UPW-aged NP had smallest sizes but were still strongly retained. Instead, the organic coating of soil-aged NP was the determining factor for the higher mobility due to steric repulsion forces.

The retention of Ag NP aged in UPW (Fig. S10) differed significantly from the retention curves obtained in a laboratory study with water-saturated sand columns by Zhang and Zhang (2014), showing almost complete breakthrough for citrate-stabilized Ag NP (particle size: 15 nm, ζ-potential: −38 mV in deionized water). This pronounced difference may be explained by the application of a completely artificial mobile phase containing only $MgSO_4$ and larger initial concentration of Ag NP (10 mg L^{-1}) in the work of Zhang and Zhang. Magnesium ions are known to have a less strongly destabilizing effect on citrate-coated Ag NP due to a lower stability of Mg-citrate complexes compared to Ca-citrate complexes (Baalousha et al., 2013; Field et al., 1975; Metreveli et al., 2015). Additionally, in our sediments the presence of a well-established biofilm can be expected in contrast to the experiments of Zhang and Zhang, as our columns are located outside and fed with natural pond water throughout the whole year. Microscopy images underline the presence of biofilm-forming organisms (i.e. diatoms) in the top sediment layer of the columns (Fig. S15). Biofilms are known to accumulate NP in natural systems (Ikuma et al., 2015). The erratically occurring peaks in our experiments may be the result of a sudden release of Ag NP aggregates from the biofilm when the biofilms got disturbed or the flow conditions changed due to natural processes (i.e. siltation) in the columns. Retention of NP in sand filters due to the presence of biofilms was already shown by Li et al. (2013). The authors compared the transport of nanoparticles through unused, biofilm-free drinking water sand filters with used sand filters having an established biofilm. They observed high breakthrough of citrate-coated Ag NP in unused sand, whereas sand which contained a biofilm reduced Ag NP breakthrough by at least 40%. Even though the authors used higher filter velocities (47 m day^{-1} as opposed to 0.2 m day^{-1} in our experiments) and much larger initial concentrations of NP (45 mg L^{-1} as opposed to 1 mg L^{-1} in our experiments) their explanation i.e. the presence of biofilms would contribute to increased retention of NP in sand filters may still be valid for our experiments. The attachment to and entrapment in biofilms in the sand column might have been one relevant retention mechanisms in our experiment. Further studies should therefore focus on this process in more detail.

Additionally, attachment to sediment surfaces and straining processes are expected to play a role for Ag NP retention in the riverbank filtration columns as shown by previous studies (such as Adrian et al., 2018; Emerson et al., 2014).

The retention mechanisms are dependent on the aging history of the Ag NP, most likely due to the change of NP surface properties. Aging in soil extract that had a larger DOC- and a lower Ca concentration than river water enhanced the colloidal stability of the Ag NP which led to a lower retention in the upper 30 cm of the sediment column. This shows that a coating layer of soil organic matter can partially inhibit the attachment of Ag NP onto grain surfaces of sand in the columns. It might also affect the interaction of the Ag NP with the biofilm as observed by Nevius et al. (2012) and Morrow et al. (2010). In contrast, the presence of high Ca concentrations during aging, such as in the river water of our study supported the NP retention. This is most likely caused by the compression of the electrical double layer of Ag NP by Ca ions leading to decreased repulsion forces in the sediment column. As Ca was also present in the pond water flushing the column, the formation of Ca-bridges between NOM-coated Ag NP and riverbank sediments might contribute to the retention.

4.3. Remobilization mechanisms from sediments

The results of our study suggest that a co-mobilization of Ag NP with Al-containing colloids was the prevailing remobilization mechanism. The majority of remobilized Ag seemed to be associated with natural colloids >1 μm. This has been reported for transport of NP in soils by previous studies (such as Hoppe et al., 2015; Makselon et al., 2017; Zhang and Zhang, 2014). As sediments of the riverbank filtration system were flushed with natural water of the surrounding pond, it is expected that organic and inorganic colloids were constantly introduced in the columns. The colloids seem to aggregate with Ag NP and were then remobilized together during batch experiments. A second possibility is that heteroaggregates were formed after remobilization. Remobilization of single Ag NP played a minor role highlighting the importance of co-mobilization of NP with natural colloids also in riverbank filtration systems and river bed sediments.

The results of the GFAAS analysis underlined that the release of Ag^+ ions was of minor importance during remobilization. As Ag^+ ions were not detected for samples remobilized in UPW and soil extract, the main part of remobilized Ag was present as particulate Ag NP, most likely attached to natural colloids > 1 μm. Nevertheless, in the presence of NH_4NO_3 Ag dissolution was observed. Due to the ecotoxicological relevance of Ag^+ ions (Beer et al., 2012), it is important to consider that retained Ag NP in sediment systems can act as a source for Ag^+ release when complexing agents such as NH_3 enter the riverbank system. However, EDX analysis of remobilized Ag NP suggest that at least partial sulfidation of Ag NP took place. This would reduce the toxicity of Ag NP to aquatic and terrestrial organisms (Lee et al., 2016; Levard et al., 2013). As sulfidation was only observed for the few NP found under the microscope it should be confirmed by further studies.

Our experiments showed that increasing mechanical forces as well as longer exposure times to these forces led to enhanced Ag remobilization, possibly through enhanced remobilization of natural, Al-containing colloids. The comparison of Ag NP remobilized in SR-NOM during 24 h of shaking and USB treatment shows that about 40% of the remobilizable Ag was only remobilized by very strong mechanical forces (Fig. S16). This was independent of the aging history of Ag NP which suggests a strong binding mechanism of this part of Ag NP to sediments that could only be disrupted by very strong mechanical forces. Of course, USB treatment results in mechanical forces much stronger than what can be found in natural systems caused by water turbulence and high flow rates. However, the application of USB treatment allowed us to determine the maximal remobilizable amount of Ag in our experiments in order to distinguish between weakly and strongly bound Ag NP.

In river systems, increasing turbulences during high-flow conditions might remobilize sediment particles and consequently also engineered NP accumulated in surficial sediment layers. Flooding events can also change hydrochemical conditions in the water phase. Those were identified as a second important factor for the remobilization of Ag NP from sediments. In the following paragraph, the determining parameters are summarized:

The presence of Ca reduced the amount of remobilizable Ag. On the one hand, Ca ions probably favored destabilization of Ag NP remobilized by strong mechanical forces and hence led to reattachment of remobilized particles. On the other hand, it most likely reduced the remobilization potential by the formation of Ca-bridges between organic matter coated NP and sediment surfaces. Liang et al. (2013) hypothesized that cation bridges enhance the interaction of Ag NP with sediment surfaces hindering the remobilization process. Moreover, at high cation concentration the energy barrier around the particle surfaces can completely disappear and the NP and their homo- and heteroaggregates can attach to the sediments irreversibly in a primary energy minimum. These mechanisms can explain the low remobilization potential observed for Ag NP aged in media with larger Ca concentrations (such as river water) as well as for Ag NP remobilized in media containing high Ca concentrations (such as soil extract).

The presence of organic matter enhanced the remobilization potential. The formation of an organic coating on the NP surface during aging in soil extract most likely led to reduced attraction forces between Ag NP and sediment grains by steric hindrance and electrostatic repulsion (Delay et al., 2011) facilitating detachment in remobilization experiments. Therefore, Ag NP aged in soil extract were remobilized to largest extents already with medium mechanical forces (i.e. 24 h of horizontal shaking). The same amount of river water- and UPW-aged Ag NP (aged in solutions with lower DOC content) was only remobilized by the strongest mechanical forces of USB treatment. However, the presence of NOM in the remobilizing medium enhanced the remobilization only when strong mechanical forces (i.e. USB treatment) were applied. While SR-NOM did not show any stronger remobilization effect during manual or horizontal shaking, it led to clearly higher remobilization during USB treatment compared to remobilization in soil extract and UPW. This suggests that NOM had an indirect remobilizing effect by stabilizing remobilized, colloidally instable Ag NP or Ag-containing natural colloids against aggregation and reattachment to sediments. Our results are in good agreement with findings of Metreveli et al. (2015) who demonstrated the important role of NOM and shear forces on the disaggregation of Ag NP homoaggregates. In their study, only strong mechanical forces (i.e. USB treatment) in combination with SR-Humic Acid caused disaggregation.

A reduction in ionic strength (i.e. remobilization in UPW) *enhanced the remobilization potential of Ag NP aged in media with higher ionic strength and DOC concentration* (i.e. river water and soil extract). Silver NP with an organic coating were most likely loosely attached in a secondary energy minimum. Those NP were remobilized by the reduction in ionic strength under soft mechanical forces since the kinetic energy of diffusion was sufficient to detach particles attached in a secondary minimum (Liang et al., 2013). Instead, more of Ag NP aged in UPW were attached to sediment surfaces in a stable primary minimum where a reduction in ionic strength is not sufficient for remobilization. This effect was only small as clay minerals and the sand as well as the NP are negatively charged at neutral pH, so that soft shear forces might have been sufficient to remobilize loosely bound Ag NP as well as Ag-containing colloids. Increasing remobilization forces (i.e. horizontal shaking and USB) then disrupted stronger bonds such as Ca bridges between NOM-coated sediment surfaces and particles leading to enhanced remobilization and overruling the effect of ionic strength reduction.

To summarize, Ag NP in sediment columns of an artificial riverbank filtration system were strongly retained and retention occurred predominantly in the top sediment layers. Sedimentation in the column head, entrapment in biofilms, aggregation and straining processes as well as adsorption to mineral surfaces are proposed to be the main retention mechanisms. Those mechanisms have a lower effect on Ag NP that experienced aging processes in soils. Instead, the retention is supported by the presence of divalent cations, such as Ca. The higher remobilization potential of soil-aged Ag NP illustrates that an aging in soil also leads to weaker bonds between NP and sediment surfaces. A combination of mechanical forces and hydrochemical changes can remobilize up to 50% of retained Ag NP. The presence of divalent cations, such as Ca reduces the remobilization potential by destabilizing Ag NP and increasing interactions between NP and sediment surfaces. According to our results, the remobilization of Ag NP predominantly takes place in the form of heteroaggregates with natural colloids larger than 1 μm while Ag^+ ions are only remobilized in the presence of strong complexing agents.

5. Conclusions

Due to a strong retention in surficial sediments, Ag NP accumulate in riverbank filtration systems where they form a potential source for the release of Ag NP and Ag^+ ions. Although the mobility of Ag NP is low, the aging of NP in soil extract can promote their breakthrough and remobilization potential. Hence, Ag NP once entering soils can form a potential source for more mobile Ag NP when they are further transported into riverbank filtration systems. There, Ag NP are retained but a remobilization is possible under changing environmental conditions. However, hydrochemical conditions alone are not enough to cause remobilization of Ag NP. The presence of moderate or strong mechanical forces which can be induced, for example, by turbulence in river systems or increasing flow velocities during flooding events, are necessary to remobilize Ag NP. The co-mobilization of Ag NP with natural clay colloids seems to be the main mechanism for remobilizing Ag from sediments of the riverbank filtration system, induced by increasing mechanical forces and the colloidal stabilization of Ag NP by NOM and ionic strength reduction.

As a potential scenario, strong precipitation events can lead to higher flow velocities, thus increasing mechanical forces and reducing the ionic strength of the surrounding solution. Additionally, flooding events might transport large amounts of NOM from floodplain soils into river systems which can then act as a stabilizing agent for the Ag NP remobilized through increasing mechanical forces. These facts suggest that even though our column experiment showed a strong retention of Ag NP in riverbank filtration systems, the potential risk of remobilization should not be neglected, although Ag concentrations are expected to be low. Nevertheless, the relevance of the identified mechanisms should be checked under more complex environmental conditions. Future studies should also focus on the effect of biofilms in sediment systems on breakthrough and remobilization, as they seem to control NP retention.

Acknowledgements

We would like to thank Natascha Volk, Iris Pieper, Silke Pabst, Lothar Beetz, Bärbel Schmidt, and Dr. Wolfgang Fey for their help and support with experiments and analysis, and Christoph Fahrenson (ZELMI TU Berlin) for SEM-EDX measurements. We thank the reviewers for their constructive comments and Dr. Ingrid Chorus for proof-reading of the manuscript.

The authors acknowledge financial support by German Research Foundation (DFG) within the research unit FOR 1536 INTERNANO and its subprojects BA 1592/6, LA 1398/9, SCHA 849/16, KA 1139/18-2, KL 2909/1-2 and VO 566/12. Anja Brandt and Kerstin Leopold are thankful to German Research Foundation (DFG) for financial support under the project LE 2457/8-1.

Appendix A. Supplementary material

Supplementary data to this article can be found online at https://doi.org/10.1016/j.scitotenv.2018.07.079.

References

Adrian, Y.F., Schneidewind, U., Bradford, S.A., Simunek, J., Fernandez-Steeger, T.M., Azzam, R., 2018. Transport and retention of surfactant- and polymer-stabilized engineered silver nanoparticles in silicate-dominated aquifer material. Environ. Pollut. 236: 195–207. https://doi.org/10.1016/j.envpol.2018.01.011.

Baalousha, M., Nur, Y., Römer, I., Tejamaya, M., Lead, J.R., 2013. Effect of monovalent and divalent cations, anions and fulvic acid on aggregation of citrate-coated silver nanoparticles. Sci. Total Environ. 454–455:119–131. https://doi.org/10.1016/j.scitotenv.2013.02.093.

Beer, C., Foldbjerg, R., Hayashi, Y., Sutherland, D.S., Autrup, H., 2012. Toxicity of silver nanoparticles—nanoparticle or silver ion? Toxicol. Lett. 208:286–292. https://doi.org/10.1016/j.toxlet.2011.11.002.

Cleveland, D., Long, S.E., Pennington, P.L., Cooper, E., Fulton, M.H., Scott, G.I., Brewer, T., Davis, J., Petersen, E.J., Wood, L., 2012. Pilot estuarine mesocosm study on the

environmental fate of silver nanomaterials leached from consumer products. Sci. Total Environ. 421–422:267–272. https://doi.org/10.1016/j.scitotenv.2012.01.025 (Special Section: Reviews of Trace Metal Pollution in China).
Coleman, J.G., Kennedy, A.J., Bednar, A.J., Ranville, J.F., Laird, J.G., Harmon, A.R., Hayes, C.A., Gray, E.P., Higgins, C.P., Lotufo, G., Steevens, J.A., 2013. Comparing the effects of nanosilver size and coating variations on bioavailability, internalization, and elimination, using *Lumbriculus variegatus*. Environ. Toxicol. Chem. 32:2069–2077. https://doi.org/10.1002/etc.2278.
Darlington, T.K., Neigh, A.M., Spencer, M.T., Guyen, O.T., Oldenburg, S.J., 2009. Nanoparticle characteristics affecting environmental fate and transport through soil. Environ. Toxicol. Chem. 28, 1191–1199.
Delay, M., Dolt, T., Woellhaf, A., Sembritzki, R., Frimmel, F.H., 2011. Interactions and stability of silver nanoparticles in the aqueous phase: influence of natural organic matter (NOM) and ionic strength. J. Chromatogr. A 1218:4206–4212. https://doi.org/10.1016/j.chroma.2011.02.074.
El Badawy, A.M., Aly Hassan, A., Scheckel, K.G., Suidan, M.T., Tolaymat, T.M., 2013. Key factors controlling the transport of silver nanoparticles in porous media. Environ. Sci. Technol. 47:4039–4045. https://doi.org/10.1021/es304580r.
Emerson, H.P., Hart, A.E., Baldwin, J.A., Waterhouse, T.C., Kitchens, C.L., Mefford, O.T., Powell, B.A., 2014. Physical transformations of iron oxide and silver nanoparticles from an intermediate scale field transport study. J. Nanopart. Res. 16 (2258). https://doi.org/10.1007/s11051-014-2258-9.
Fang, J., Wang, M., Lin, D., Shen, B., 2016. Enhanced transport of CeO 2 nanoparticles in porous media by macropores. Sci. Total Environ. 543:223–229. https://doi.org/10.1016/j.scitotenv.2015.11.039.
Feichtmeier, N.S., Leopold, K., 2014. Detection of silver nanoparticles in parsley by solid sampling high-resolution–continuum source atomic absorption spectrometry. Anal. Bioanal. Chem. 406:3887–3894. https://doi.org/10.1007/s00216-013-7510-0.
Ferry, J.L., Craig, P., Hexel, C., Sisco, P., Frey, R., Pennington, P.L., Fulton, M.H., Scott, I.G., Decho, A.W., Kashiwada, S., Murphy, C.J., Shaw, T.J., 2009. Transfer of gold nanoparticles from the water column to the estuarine food web. Nat. Nanotechnol. 4:441–444. https://doi.org/10.1038/nnano.2009.157.
Field, T.B., Coburn, J., McCourt, J.L., McBryde, W.A.E., 1975. Composition and stability of some metal citrate and diglycolate complexes in aqueous solution. Anal. Chim. Acta 74, 101–106.
Furtado, L.M., Norman, B.C., Xenopoulos, M.A., Frost, P.C., Metcalfe, C.D., Hintelmann, H., 2015. Environmental fate of silver nanoparticles in boreal lake ecosystems. Environ. Sci. Technol. 49:8441–8450. https://doi.org/10.1021/acs.est.5b01116.
Hoppe, M., Mikutta, R., Utermann, J., Duijnisveld, W., Kaufhold, S., Stange, C.F., Guggenberger, G., 2015. Remobilization of sterically stabilized silver nanoparticles from farmland soils determined by column leaching: remobilization of silver nanoparticles from soil. Eur. J. Soil Sci. 66:898–909. https://doi.org/10.1111/ejss.12270.
Ikuma, K., Decho, A.W., Lau, B.L.T., 2015. When nanoparticles meet biofilms-interactions guiding the environmental fate and accumulation of nanoparticles. Front. Microbiol. 6. https://doi.org/10.3389/fmicb.2015.00591.
Klitzke, S., Metreveli, G., Peters, A., Schaumann, G.E., Lang, F., 2015. The fate of silver nanoparticles in soil solution — sorption of solutes and aggregation. Sci. Total Environ. 535: 54–60. https://doi.org/10.1016/j.scitotenv.2014.10.108.
Lee, S.-W., Park, S.-Y., Kim, Y., Im, H., Choi, J., 2016. Effect of sulfidation and dissolved organic matters on toxicity of silver nanoparticles in sediment dwelling organism, *Chironomus riparius*. Sci. Total Environ. 553:565–573. https://doi.org/10.1016/j.scitotenv.2016.02.064.
Levard, C., Hotze, E.M., Colman, B.P., Dale, A.L., Truong, L., Yang, X.Y., Bone, A.J., Brown, G.E., Tanguay, R.L., Di Giulio, R.T., Bernhardt, E.S., Meyer, J.N., Wiesner, M.R., Lowry, G.V., 2013. Sulfidation of silver nanoparticles: natural antidote to their toxicity. Environ. Sci. Technol. 47:13440–13448. https://doi.org/10.1021/es403527n.
Li, Z., Aly Hassan, A., Sahle-Demessie, E., Sorial, G.A., 2013. Transport of nanoparticles with dispersant through biofilm coated drinking water sand filters. Water Res. 47: 6457–6466. https://doi.org/10.1016/j.watres.2013.08.026.
Liang, Y., Bradford, S.A., Simunek, J., Vereecken, H., Klumpp, E., 2013. Sensitivity of the transport and retention of stabilized silver nanoparticles to physicochemical factors. Water Res. 47:2572–2582. https://doi.org/10.1016/j.watres.2013.02.025.
Lowry, G.V., Gregory, K.B., Apte, S.C., Lead, J.R., 2012. Transformations of nanomaterials in the environment. Environ. Sci. Technol. 46:6893–6899. https://doi.org/10.1021/es300839e.
Lv, X., Gao, B., Sun, Y., Dong, S., Wu, J., Jiang, B., Shi, X., 2016. Effects of grain size and structural heterogeneity on the transport and retention of nano-TiO2 in saturated porous media. Sci. Total Environ. 563–564:987–995. https://doi.org/10.1016/j.scitotenv.2015.12.128.
Makselon, J., Zhou, D., Engelhardt, I., Jacques, D., Klumpp, E., 2017. Experimental and numerical investigations of silver nanoparticle transport under variable flow and ionic strength in soil. Environ. Sci. Technol. 51:2096–2104. https://doi.org/10.1021/acs.est.6b04882.
Meakin, P., 1988. Fractal aggregates. Adv. Colloid Interface Sci. 28:249–331. https://doi.org/10.1016/0001-8686(87)80016-7.
Metreveli, G., Philippe, A., Schaumann, G.E., 2015. Disaggregation of silver nanoparticle homoaggregates in a river water matrix. Sci. Total Environ. 535:35–44. https://doi.org/10.1016/j.scitotenv.2014.11.058.
Morrow, J.B., Arango, C.P., Holbrook, R.D., 2010. Association of quantum dot nanoparticles with biofilm. J. Environ. Qual. 39:1934–1941. https://doi.org/10.2134/jeq2009.0455.
Nel, A., Xia, T., Mädler, L., Li, N., 2006. Toxic potential of materials at the NANOLEVEL. Science 311:622–627. https://doi.org/10.1126/science.1114397.
Neukum, C., Braun, A., Azzam, R., 2014. Transport of engineered silver (Ag) nanoparticles through partially fractured sandstones. J. Contam. Hydrol. 164:181–192. https://doi.org/10.1016/j.jconhyd.2014.05.012.
Nevius, B.A., Chen, Y.P., Ferry, J.L., Decho, A.W., 2012. Surface-functionalization effects on uptake of fluorescent polystyrene nanoparticles by model biofilms. Ecotoxicology 21: 2205–2213. https://doi.org/10.1007/s10646-012-0975-3.
Philippe, A., Schaumann, G.E., 2014. Interactions of dissolved organic matter with natural and engineered inorganic colloids: a review. Environ. Sci. Technol. 48:8946–8962. https://doi.org/10.1021/es502342r.
Philippe, A., Gangloff, M., Rakcheev, D., Schaumann, G.E., 2014. Evaluation of hydrodynamic chromatography coupled with inductively coupled plasma mass spectrometry detector for analysis of colloids in environmental media – effects of colloid composition, coating and shape. Anal. Methods 6:8722–8728. https://doi.org/10.1039/C4AY01567C.
Praetorius, A., Labille, J., Scheringer, M., Thill, A., Hungerbühler, K., Bottero, J.-Y., 2014. Heteroaggregation of titanium dioxide nanoparticles with model natural colloids under environmentally relevant conditions. Environ. Sci. Technol. 48:10690–10698. https://doi.org/10.1021/es501655v.
Sagee, O., Dror, I., Berkowitz, B., 2012. Transport of silver nanoparticles (AgNPs) in soil. Chemosphere 88:670–675. https://doi.org/10.1016/j.chemosphere.2012.03.055.
Schaumann, G.E., Philippe, A., Bundschuh, M., Metreveli, G., Klitzke, S., Rakcheev, D., Grün, A., Kumahor, S.K., Kühn, M., Baumann, T., Lang, F., Manz, W., Schulz, R., Vogel, H.-J., 2015. Understanding the fate and biological effects of Ag- and TiO2-nanoparticles in the environment: the quest for advanced analytics and interdisciplinary concepts. Sci. Total Environ. 535:3–19. https://doi.org/10.1016/j.scitotenv.2014.10.035.
Schlich, K., Hoppe, M., Kraas, M., Fries, E., Hund-Rinke, K., 2017. Ecotoxicity and fate of a silver nanomaterial in an outdoor lysimeter study. Ecotoxicology 26:738–751. https://doi.org/10.1007/s10646-017-1805-4.
Schmidt, C.K., Lange, F.T., Brauch, H.-J., Kühn, W., 2003. Experiences With Riverbank Filtration and Infiltration in Germany. p. 17.
Selck, H., Handy, R.D., Fernandes, T.F., Klaine, S.J., Petersen, E.J., 2016. Nanomaterials in the aquatic environment: a European Union-United States perspective on the status of ecotoxicity testing, research priorities, and challenges ahead: nanomaterials in the aquatic environment. Environ. Toxicol. Chem. 35:1055–1067. https://doi.org/10.1002/etc.3385.
Sprenger, C., Hartog, N., Hernández, M., Vilanova, E., Grützmacher, G., Scheibler, F., Hannappel, S., 2017. Inventory of managed aquifer recharge sites in Europe: historical development, current situation and perspectives. Hydrogeol. J. 25:1909–1922. https://doi.org/10.1007/s10040-017-1554-8.
Turkevich, J., Stevenson, P.C., Hillier, J., 1951. A study of the nucleation and growth processes in the synthesis of colloidal gold. Discuss. Faraday Soc. 11:55. https://doi.org/10.1039/df9511100055.
Vance, M.E., Kuiken, T., Vejerano, E.P., McGinnis, S.P., Hochella, M.F., Rejeski, D., Hull, M.S., 2015. Nanotechnology in the real world: redeveloping the nanomaterial consumer products inventory. Beilstein J. Nanotechnol. 6:1769–1780. https://doi.org/10.3762/bjnano.6.181.
Zhang, H., Zhang, C., 2014. Transport of silver nanoparticles capped with different stabilizers in water saturated porous media. 6.
Zirkler, D., Lang, F., Kaupenjohann, M., 2012. "Lost in filtration"—the separation of soil colloids from larger particles. Colloids Surf. A Physicochem. Eng. Asp. 399:35–40. https://doi.org/10.1016/j.colsurfa.2012.02.02.